Symbiosis

www.symbiosisonline.org
www.symbiosisonlinepublishing.com

Research Article | International Journal of Molecular and Theoretical Physics | Open Access

Understanding the nature of Metal Oxalato Complexes with Purine Nucleobase- A Quantum Chemical approach

Palanisamy Deepa*

**Department of Physics, Manonmaniam Sundaranar University, Tirunelveli, India.*

Received: March 14, 2017; Accepted: April 10, 2017; Published: April 18, 2017

***Corresponding author:** Palanisamy Deepa, Department of Physics, Manonmaniam Sundaranar University, Tirunelveli, India. Pin- 627 012, Tel: 91-9952372140; E-mail: phydeepa09@gmail.com*

Abstract

Crystal structures of {[Cd(μ-ox) (H ade) (H_2O)]. H_2O}n, {[Cu(μ-ox) (3Meade) (H_2O)].H_2O}n and {[Cu(ox) (H_2O)$_2$(9Megua)].2.5H_2O}n complexes are linked by bidentate oxalato ligands. Density functional theory calculation has been performed on the above complexes to investigate their electronic structures and to explore the stability of the monomer and complexes. The geometrical parameters calculated by DFT method are found to have reasonably good agreement with the x-ray crystallographic data. The investigation includes a variety of theoretical analyses such as interaction energy, electrostatic potential map, topological, NBO, and NMR analyses. The present calculations provide an important physicochemical insight into the structure and properties of metal oxalato ligands, 3 methyl adenine and 9-methyl guanine. The results help to understand the active role of coordinated water molecules in modulating the binding of the oxalato ligands through hydrogen bonds.

Keywords: Bidentate oxalato ligands; Density functional theory; Interaction energy; Electrostatic potential map; Topological analysis;

Introduction

For the past few decades many research efforts have been examined to understand the binding properties of nucleic acids and their constituents with metal ions, which aid to develop the new biologically active metallo drug. The interaction of DNA/RNA constituents and their derivatives with both organic and inorganic molecules help to design the biomimetic systems [1-4] and the development of artificial nucleobase receptors used as specific nucleotide sensors [5]. Plenty of structural studies concerning metal complexes with purine-like ligands are focused on mixed-ligand metal complexes, where the metal binding pattern is deliberated for the configuration of a M-N (purine) bond, in some cases it is reinforced by a suitable intra-molecular interligand hydrogen bonding interaction [6-12]. Owing to the increasing interest in the non-bonding interactions (hydrogen bonds [13], π,π-stacking [14, 15] and C–H/π interactions [16,17]), our attention determined to examine their behaviour in the metal-ligand interaction, intramolecular and inter molecular ligand interactions. These are the cases of a variety of ternary metal complexes involving Nucleobases [9-11] and the metal ion binding pattern is targeted as the main goal.

Galindo, et al. [2] have reported a model for metal ion-DNA interactions and molecular architecture of metal complexes capable of forming base-pair hydrogen bonding. Garcia-Teran, et al. [18] have characterized three M(II) oxalato complexes containing the adenanium nucleobase. Dance, et al. [19] have demonstrated the importance of extended structures with metal building blocks based on the use of intermolecular forces such as hydrogen bond and /or π-π interactions. Sonia Perez-Yanez, et al. [20] have studied the metal oxalato and malanato systems, which act as receptors of adenine and cytosine by means of the covalent anchoring of nucleobases to the metal centers [18, 21-23]. They have synthesized and reported the supramolecular structure of compounds {[Cd(μ-ox) (H ade) (H_2O)]. H_2O}n, {[Cu(μ-ox) (3Meade) (H_2O)].H_2O}n and {[Cu(ox)(H_2O)$_2$(9Megua)].2.5H_2O}n n, containing the non-modified adenine nucleobase (H ade), the 3 methyl adenine (3 me ade) and the model 9-methyl guanine (9 me gua) which act as monodentate ligands. The 3 methyl adenine is highly cytotoxic and mutageni, since it can able to arrest the replication of DNA, where the methyl group N3 project into the minor groove of DNA double helix and thereby prevent the replication [24]. Hence, the design and structural analyses of coordination compounds containing the methylated adenine can able to predict useful information, which assist to understand the conformational damages induced through the nucleobase alkylation in biological systems and the molecular identification procedure to restore them.

In the present study an attempt has been made to recognize the structural behavior and characteristic properties of crystal compounds **{[Cd(μ-ox) (H ade) (H_2O)]. H_2O}n, {[Cu(μ-ox) (3Meade) (H_2O)].H_2O}n and {[Cu(ox) (H_2O)$_2$(9Megua)].2.5H_2O}n,** with CCDC numbers: 779251, 779252 and 779253 by using density functional theory by employing LANL2DZ basis set. We are interested to examine the binding strength formed through hydrogen bonds in through mixed-metal ligand and hence the crystal compounds have been

investigated through two ways i). Hydrogen bonding arrangement and ii). Stacking arrangement. In extension to our previous work on the interaction of biomolecules with water [25], drugs [26-29] and metal ions [30-32], this work is concerned with the investigation of available X-ray crystallographic data [20] with the results of the theoretical methods. In order to know the potency of mixed-metal-ligand binding and the influence of water molecules on their binding affinity the interaction energy calculations have been examined for the hydrogen bonding and stacking arrangement. The active sites of heavy atoms responsible for the binding strength in hydrogen bonding and π-π stacking of supramolecular architecture for all the complexes were analyzed using electrostatic potential map. The role of individual hydrogen bonds and their contribution for the stable nature was analyzed through AIM and NBO analyses. The nature of hydrogen atoms was examined through NMR chemical shift.

Computational Methodology

The crystal compounds of all the complexes used in this work were extracted from the Cambridge Crystal Structure Database (CCSD) and the molecular geometries of {[Cd(μ-ox) (H ade) (H_2O)]. H_2O}n, {[Cu(μ-ox) (3Meade) (H_2O)].H_2O}n and {[Cu(ox)(H_2O)$_2$(9Megua)].2.5H_2O}n, monomers and their complexes were fully optimized using the Density functional theory at B3LYP and M05 [33] levels of theory with LANL2DZ basis set. The choice of the LANL2DZ basis set for metal complexes is based on the accurate results obtained for metal–ligand interactions [34, 35]. The vibrational frequency analysis computed for all the optimized structures reveal the structures are observed with real local minima and no structures are found with imaginary frequencies. The interaction (binding) energies of all the hydrogen bonding and stacking arrangement of the complexes are corrected using a Counterpoise correction [36] to a basis set superposition error. **The interaction energies were performed for these complexes by using the formula:**

$$\Delta^2 E(AB) = E_{AB} - [E_{(A)} + E_{(B)}] \quad (1)$$

where E(AB) is the total energy of two monomers and EA, EB, are the total energy of individual monomer. Note that while calculating interaction energies the BSSE was corrected.

In turn to accomplish an extra precise energy evaluation between the metal-ligand complexes considered, single point interaction energy calculation at MP2/LANL2DZ level of theory was performed for the optimized geometries at M05/LANL2DZ level of theory. To confirm the presence of hydrogen bonding a topological analysis has been carried out to calculate the charge density ρ(r) and its second derivative Laplacian of charge density $\nabla^{2\rho(r)}$ for bonds using Baders Atoms in molecules (AIM) theory [37-41]. The NBO analysis has also been carried out for all the molecules using the same level of theory employing the NBO 3.1 Program [42]. Electrostatic potential maps have been produced for the monomer and complexes. NMR calculations have been carried out for all the complexes based on the Cheeseman coworkers [43] method at M05/LANL2DZ level of theory, where isotropic H values are taken into account. All the calculations have been performed using Gaussian 09 W package [44].

Results and Discussion

Interatomic distances

The experimental crystalline atomic coordinates of {[Cd(μ-ox) (H ade) (H_2O)]. H_2O}n, {[Cu(μ-ox) (3Meade) (H_2O)]. H_2O}n and {[Cu(ox)(H_2O)$_2$(9Megua)].2.5H_2O}n,,complexes were used as the starting point for geometry optimization, and protonation has been included at the end of oxalato group for ideal geometries. All the complexes were optimized at B3LYP/LANL2DZ and M05/LANL2DZ levels of theory and are given in Figures. 1-3.

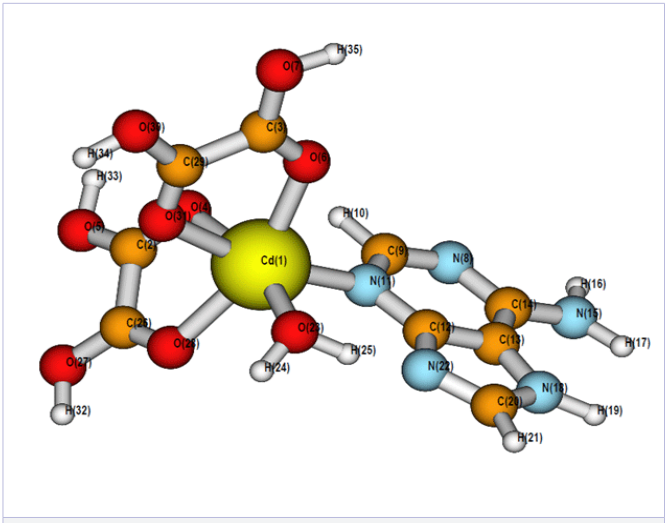

Figure 1a : Monomer

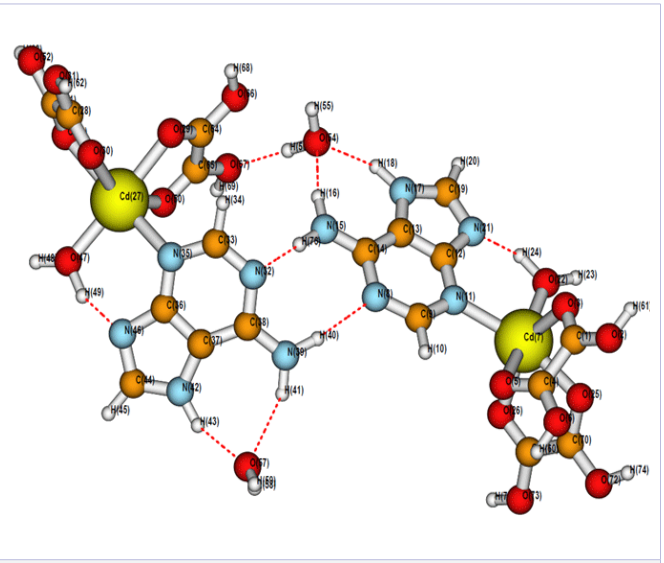

Figure 1b : Hydrogen bonding arrangement

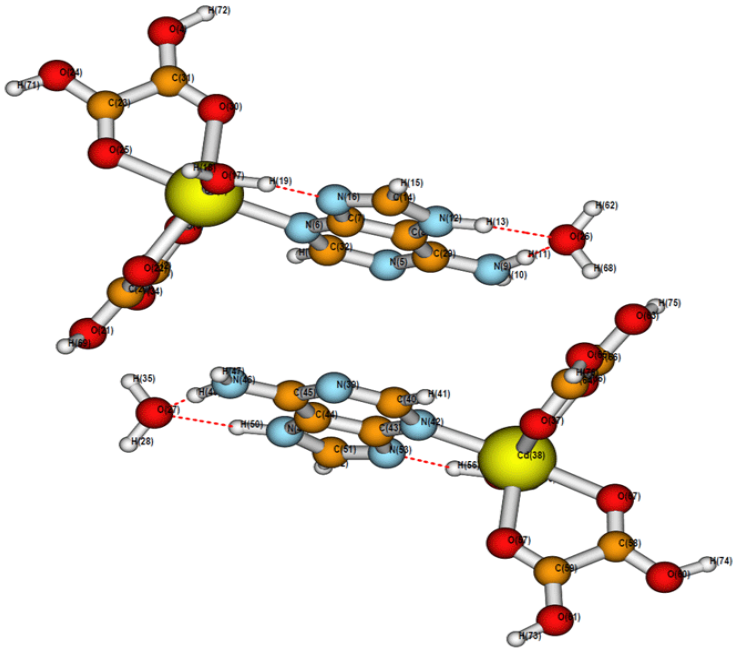

Figure 1b :
Figure 1: The optimized a).Monomer b). Hydrogen bonding arrangement c). Stacking arrangement of {[Cd(μ-ox) (H ade) (H_2O)]. H_2O}n at M05/LANL2DZ level of theory

Table 1: Comparison of bond distance (Å) and bond angles of monomers (Complex 1, Complex 2 and Complex 3) optimized at B3LYP/LANL2DZ and M05/LANL2DZ levels of theory with the available crystallographic data.

Bonding	Complex-1			Complex -2			Complex -3		
	B3LYP	MO5	EXP	B3LYP	MO5	EXP	B3LYP	MO5	EXP
M - N_{11}	2.297	2.288	2.281	-	-	-	-	-	-
M - O(w)	2.295	2.201	2.284	2.160	2.176	2.223	-	-	-
M - O_6	2.340	2.472	2.292	2.063	1.943	1.984	-	-	-
M - O_3	2.295	2.424	2.269	1.947	2.090	2.038	-	-	-
M - O_{28}(w)	-	-	-	-	-	-	2.104	2.125	2.341
M - O_4	2.295	2.439	2.296	2.229	2.344	2.038	-	-	-
M - O_{28}	2.340	2.451	2.338	2.487	2.421	2.382	-	-	-
M - N_{19}	-	-	-	2.050	2.021	1.989	2.036	2.107	1.997
M - O_{27}(w)	-	-	-	-	-	-	2.156	2.189	1.945
∠N_{11}-M-O_3	99.55	110.24	99.45	-	-	-	-	-	-
∠N_{22}-M-O_{30}	-	-	-	99.86	98.90	95.970	-	-	-
∠N_{11}-M-O_{28}(w)	91.48	92.11	90.95	-	-	-	-	-	-
∠N_{22}-M-O_{26}(w)	-	-	-	92.93	90.71	95.243	-	-	-
∠N_{19}-M-O_{28}(w)	-	-	-	-	-	-	107.12	104.45	93.24
∠N_{17}-M-O_{27}(w)	-	-	-	-	-	-	101.59	99.47	94.65
ϑ O_3-M-N_{11}-C_9	83.75	82.41	94.080	-	-	-	-	-	-
JO_4-M-N_{11}-C_2	103.29	102.91	103.76	-	-	-	-	-	-
JO_{30}-M-N_{22}-C_{28}	-	-	-	65.74	68.20	53.553	-	-	-
JO_2–M-N_{22}–C_{23}	-	-	-	161.70	162.47	152.90	-	-	-
JO_3–M-N_{19}–C_{16}	-	-	-	-	-	-	126.39	128.62	-
JO_{27}–M-N_{19}–C_{16}	-	-	-	-	-	-	177.20	177.31	-
JO_{28}–M-N_{19}–C_{16}	-	-	-	-	-	-	44.38	44.14	-

Table 2: Comparison of hydrogen bond lengths H…Y (Å) of the metal interacting complexes (hydrogen bonding and stacking arrangement) at B3LYP/LANL2DZ and M05/LANL2DZ levels of theory with the available crystallographic data and Stabilization Energy (E^2) kcal/mol at M05/LANL2DZ from NBO analysis.

Bonding	B3LYP	MO5	Experimental	$E^{(2)}$
Hydrogen Bond Arrangement				
Complex 1				
N_{39}-H_{40}…N_{8}	2.188	2.088	2.239	9.98
N_{15}-H_{76}…..N_{32}	1.867	1.769	2.239	23.89
N_{39}-H_{41}…..O_{57w}	2.127	2.163	2.308	5.55
N_{42}-H_{43}…..O_{57w}	1.814	1.793	1.971	19.09
N_{15}-H_{16}…O_{54w}	1.939	1.899	2.308	9.64
N_{17}-H_{18}…O_{54w}	1.808	1.842	1.971	10.97
O_{22w}-H_{24}….N_{21}	1.669	1.537	1.939	62.30
O_{54w}-H_{56}…O_{67}	1.788	1.807	-	12.14
O_{47w}-H_{49}….N_{46}	1.623	1.564	1.939	55.48
O_{54w}-H_{55}…O_{66}	2.433	2.370	-	0.83
Complex 2				
N_{26}-H_{55}…O_{38}	1.978	2.323	2.011	1.26
N_{26}-H_{68}…..O_{20}	2.018	2.159	2.201	2.47
N_{11}-H_{64}…..O_{23}	1.912	2.069	2.011	1.14
C_{5}-H_{65}….N_{28}	2.013	2.299	2.806	2.93
Complex 3				
O_{27}-H_{29}…O_{50}	1.905	2.212	1.796	12.68
N_{40}-H_{41}……O_{3}	1.941	2.023	2.046	5.69
N_{43}-H_{45}….O_{4}	2.176	1.829	2.021	4.02
Stacking Arrangement				
Complex 1				
N_{46}-H_{48}…O_{27w}	2.212	1.909	2.308	9.43
N_{49}-H_{50}…O_{27w}	1.634	1.910	1.971	7.94
O_{54}-H_{56}…N_{53w}	1.623	1.529	1.939	64.91
N_{12}-H_{13}…O_{26w}	1.634	1.910	1.971	7.95
N_{9}-H_{11}…O_{26w}	2.210	1.909	2.308	9.43
O_{17}-H_{19}…N_{16w}	1.621	1.529	1.939	64.91
Complex 2				
N_{22}-H_{24}…O_{31}	1.987	2.165	2.011	3.11
O_{2w}-H_{28}…N_{40}	2.523	2.676	-	2.54
N_{1}-H_{52}…O_{61}	1.972	2.209	2.011	10.39
O_{57w}-H_{58}…N_{11}	1.812	1.878	-	-

The Table 1 and 2 compares the results of geometrical parameters and hydrogen bond lengths calculated by theoretical and experimental methods for all the three complexes. In the present study, in order to occur more structural details the complexes were divided into two categories based on hydrogen bonding and stacking arrangement. {[Cd(μ-ox) (H ade) (H_2O)]. H_2O}n, {[Cu(μ-ox) (3Meade) (H_2O)].H_2O}n and {[Cu(ox) (H_2O)$_2$(9Megua)].2.5H_2O}n, were named as complex 1, complex 2 and complex 3 respectively.

i) {[Cd(μ-ox) (H ade) (H2O)]. H2O}n: As seen from, it is renowned that the metal atoms display an unclear octahedral arrangement produced by four oxygen atoms as of two connecting oxalato ligands, a single water molecule and a nitrogen atom having endocylic property of the adenine ring. This complex proliferates to form the 1D zig-zag chain, where the nucleobase is coordinated perpendicular to the propagating direction [20]. In

case of monomer the M-O (M=Cd) bond distance originates from 2.29 to 2.34 Å and 2.20 to 2.47 Å, where the adenine nucleobase bonded through N11 atom has the M-N11 bond distance of 2.29 Å and 2.28 Å at B3LYP and M05 levels of theory respectively. This agrees well with the experimental crystal data and the previously reported values of **crystal** compound [20, 45, 46]. The dihedral angle between two consecutive oxalato bridging ligands (O_3-Cd_1-O_4-C_2) are 82.27° and 81.16° at above levels of theory respectively which were underestimated by 7° compared to those observed in X-ray crystallography. The dihedral angle between the adenine moiety and the oxalato ligands O_6-Cd1-N_{11}-C_9 is 103.29° and 102.91° at the above levels of theory respectively, which are in agreement with the experimental value of 103.76°.

While considering the {[Cd(μ-ox) (H ade) (H2O)]. H2O} n complex, it is renowned that inter and intramolecular hydrogen bonds were created in hydrogen bonding arrangement. From the Table 2 it is observed that from the metal oxalato complex containing adenine nucleobase the intra molecular hydrogen bond length (Ade O22-H24….. N21 (W)) is 1.66 Å and 1.53 Å at the above levels of theory respectively which is underestimated by crystallography data of 0.3 Å. The intermolecular hydrogen bond length plays a significant contribution in the configuration of polymeric chain compound [20]. The nucleobase of the two polymeric chains be interlinked by hydrogen bonding interaction between two Watson-crick faces of two nucleobases and is shown in Figure. 1b.

. In the complex, the adenine ligands are oriented in such a way to form an intramolecular hydrogen bond involving the coordinated water molecule (donor) and the N46 atom (acceptor), which strengthen the observed metal-binding pattern of the nucleobase [20]. Furthermore, the proton transfer from N_{46} to N_{42} atom favors the formation of a hydrogen bond between the Hoogsteen face [N_{39}, N_{42}] of the nucleobase as donor and a crystallization water molecule as acceptor with asymmetric N…O distances of 3.12 Å and 2.77 Å at the above levels of theory. These values agree with the experimental values. The π-π stacking between adenine base of the {[Cd(μ-ox) (H ade) (H_2O)]. H_2O}n complex is so long to form face to face or edge to face interaction between the π system, but the coordinated nucleobases establishes π-π stacking of the above complex and is shown in Figure. 1c. The distance between two adjacent stacked nucleobase is 3.52 Å and 3.64 Å at B3LYP and MO5 levels of theory, which is comparable with the experimental value of 3.6 Å. Moreover the interaction energy observed for hydrogen bonding and stacking arrangement is -71.58, -77.63, -77.53 and -60.23, -59.98, -65.48 kcal/mol at B3LYP, MO5 and MP2 levels of theory indicating the stability and strength of the interaction.

ii). {[Cu(μ-ox) (3Meade) (H2O)].H2O}n: As seen from the Figure. 2a, in case of monomer, the fragments are joined by bis-bidentate oxalato ligands. The metal centre exhibits a tetragonally elongated $CuNO_{30}O_{26}$w chromophore wherein three oxygen atoms of two oxalato ligands is in the equatorial plane and the imidazole N_{22} atom of the 3-methyl adenine20. The apical positions of the octahedral coordination are filled by the remaining O_7 oxygen atom of the oxalato bridging ligand and the O_{26}w coordinated water molecule with calculated metal-ligand bond distances are 2.16 Å and 2.17 Å at B3LYP and M05 levels of theory respectively. The perpendicular position of 3-methyl adenine with metal oxalato arrangement permits the establishment of face-to-face π-π interactions between adjacent pyrimidinic rings. For monomer, the bond length of Cu1-O_{26}(w) is 2.16 Å and 2.17 Å, and for metal coordinated oxygen atom, it is 1.94 to 2.48 Å and 1.94 to 2.42 Å at above levels of theory respectively, which agree well with the x-ray crystallographic data. The adenine base coordinated to the metal atom by N_{22} and the bond distance of Cu1-N_{22} is 2.05 Å (B3LYP), 2.021 Å (MO5) and the experimental value is 1.98 Å. The layers of polymeric chains are held together by an intricate network of hydrogen bonding interactions and are given in Figure. 2b. The Watson-Crick face of the nucleobases form a layer by hydrogen bond to the adjacent ones by means of a N_{26}–H_{68}…O20 (1.986, 2.159Å) and N_{26}–H_{55}…O_{38} (1.914, 2.323Å) interaction between the exocyclic amino group and the oxalato ligand, and by a weak C5–H65…N28 (2.013, 2.299Å) base-base association.

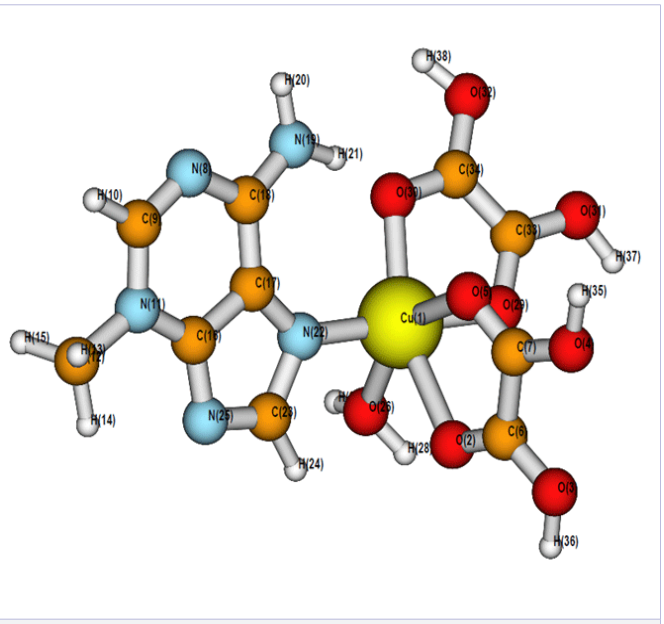

Figure 2a : Monomer

The N_{35} nitrogen atom of the imidazole ring acts as acceptor of a hydrogen bonding interaction with the coordinated water molecule of a neighbouring chain (Figure. 2b). The stacking arrangement of the above complex is shown in Figure. 2c and their stacking distance is 4.37 Å and 4.13Å at the above levels of theory respectively. Finally the interaction energy for hydrogen bonding and stacking arrangement is -54.35, -56.34, -55.82 and -45.31, -47.35, 48.58 kcal/mol at B3LYP, M05 and MP2 levels of theory, which influences the stability of the structure.

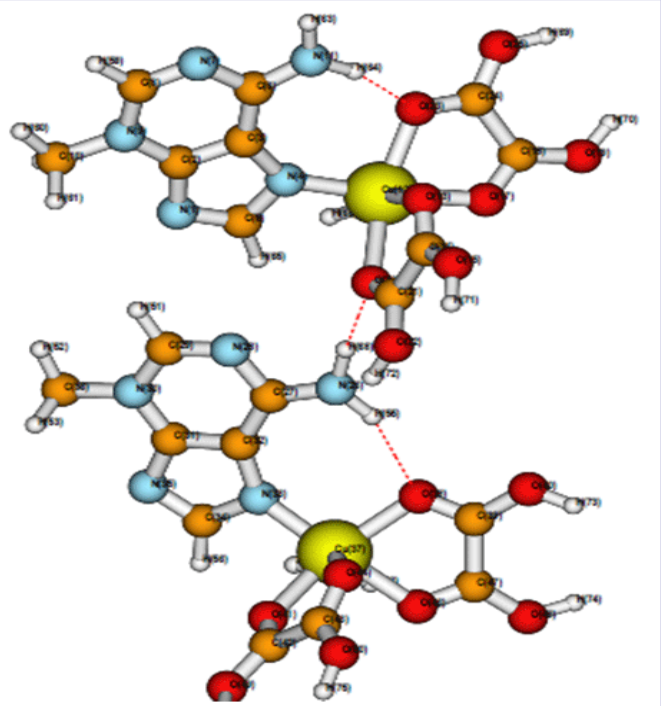

Figure 2b : Hydrogen bonding arrangement

is 4.37 Å and 4.13Å at the above levels of theory respectively. Finally the interact

iii).{[Cu(ox)(H2O)2(9Megua)].2.5H2O}n: The supramolecular structure of {[Cu(ox)(H_2O)$_2$(9Megua)].2.5H_2O}n complex is quite different from the above complexes and the optimized structures are shown in Figure. 3.

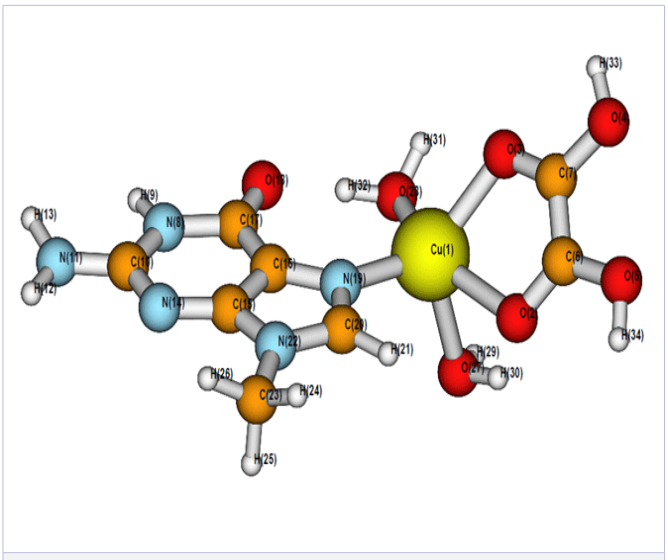

Figure 3a : Monomer

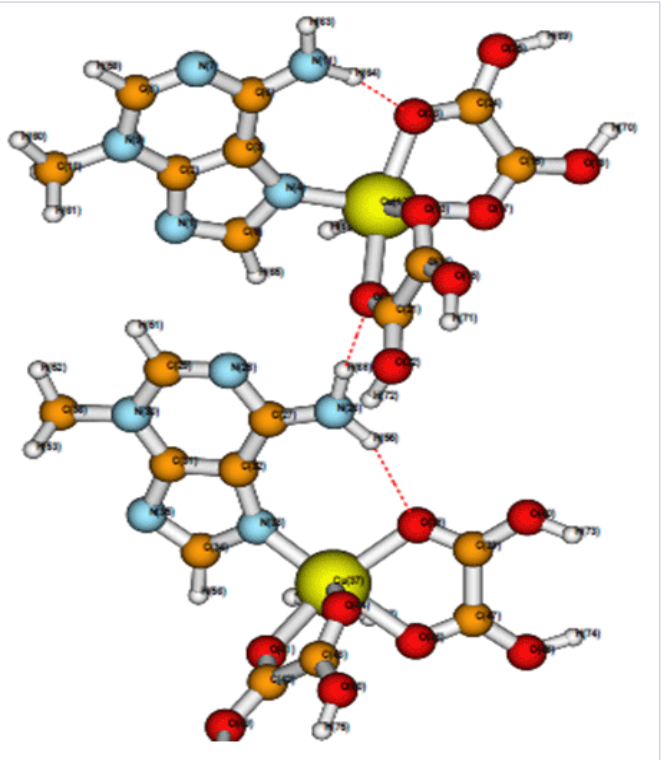

Figure 2c : Stacking arrangement
Figure 2: The optimized a).Monomer b). Hydrogen bonding arrangement c). Stacking arrangement of {[Cu(μ-ox) (3Meade) (H_2O)].H_2O}n at M05/LANL2DZ level of theory

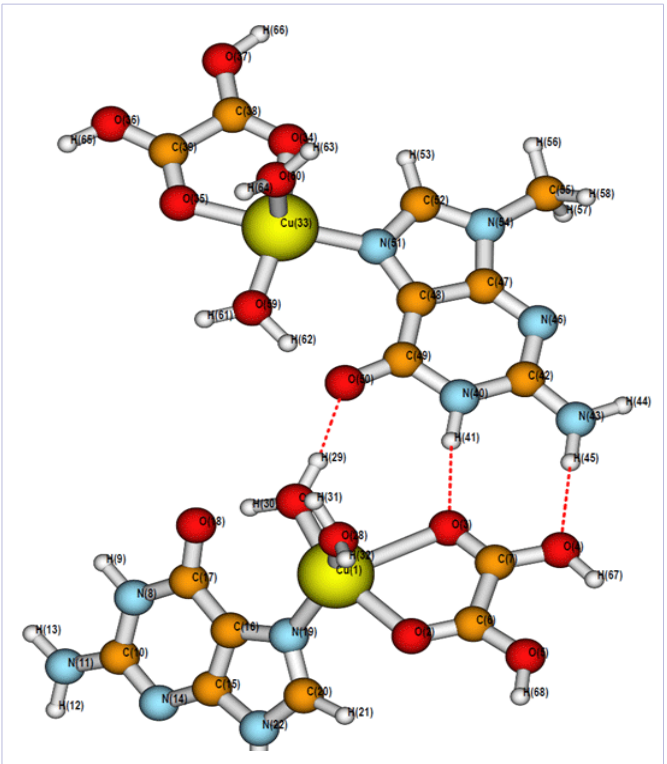

Figure 3b : Hydrogen bonding arrangement
Figure 3: The optimized monomer a).Monomer b). Hydrogen bonding arrangement of {[Cu(ox)(H2O)2(9Megua)].2.5H2O}n at M05/LANL2DZ level of theory

The metal core assume a indistinct square pyramidal nature coordination, wherein the basal plane is engaged by two oxygen atoms from a bidentate oxalato ligand, one water molecule , and the nucleobase having N_{19} site is the most common coordination metal binding model intended for the 9-methylguanine ligand [20]. In case of monomer the apical positions occupied by water molecules with Cu-O_{28}w distance is 2.15 Å and 2.18 Å at B3LYP and MO5 levels of theory respectively. As observed from Figure. 3b the Watson-Crick face of the nucleobase establishes a triple hydrogen bonding interaction with three oxygen atoms, one from the coordinated water molecule and the other ones from a carboxylate group of the oxalato ligand. The metal to oxygen Cu-O_{28}w bond length is 2.10 Å and 2.12 Å at B3LYP and M05 levels of theory respectively, which underestimates the experimental value around 0.2 Å. The guanine base is coordinated by Cu-N_{19} bond and the bond length is 2.03 Å and 2.10 Å at the above levels of theory respectively which overestimates by 0.1 Å. The keto group of the guanine ligand establishes an intramolecular hydrogen bond with the coordinated water molecule, where the N8H9 and $N_{11}H_{13}$ sites are connected to the non-coordinated oxygen atoms from an adjacent unit to form hydrogen bonded motif. In this complex O_{27}-H_{29}.....O_{50} interaction is 1.90 Å, 2.21 Å at above levels of theory respectively, which is overestimated by 2-4 Å. The interaction energy of the complex is -13.17, -8.13 and -18.23 kcal/mol at B3LYP, M05 and MP2 levels of theory indicating the strength of the interaction.

Electrostatic potential map

The electrostatic potentials (ESPs) disclose the significant contribution on the structural behaviour and properties of the considered metal-ligand complexes. In general Electrostatic property of nucleotides rule the directional behaviour of stacking interactions and this is vital for the dependability of DNA polymerase. Chin, et al. [47] proposed that the electrostatic potential will give a reliable contribution in understanding the nature of each individual atoms in nucleic acid identification and stabilization. The position of abnormal electrostatic features reveals the importance of functional regions, for instance, the binding spot intended for the metal ions are characterized by a typically negative electrostatic potential. The electrostatic potential maps was drawn for the monomers and complexes and are shown in Figures 4 and 5, where the red regions stand for the most electron rich regions and blue region correspond to the most electron poor region of the monomers. The projection of the electrostatic potential on the 0.0004 a.u electron density surface clearly shows noteworthy concentration of the negative charge around metal oxalato atoms. The overlapping of the charges between electronegative atoms and metal atoms in the complexes decreases from Cu to Cd complexes.

Topological and NBO analysis

To gain further insight into the nature of hydrogen bond in the metal complexes, we have performed the electron density based topological analysis within the framework of

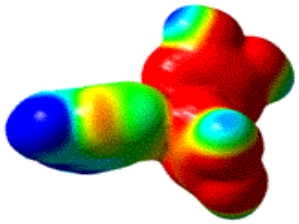

{[Cd(μ-ox) (H ade) (H2O)]. H2O}n (Monomer -1)

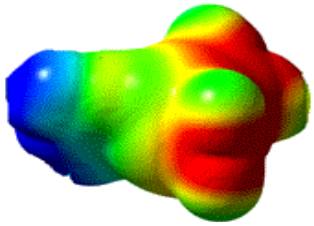

{[Cu(μ-ox) (3Meade) (H2O)].H2O}n (Monomer -2)

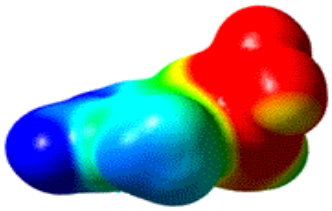

{[Cu(ox)(H2O)2(9Megua)].2.5H2O}n (Monomer -3)

Figure 4: Electrostatic potential of the monomers 1to 3 mapped onto the surface of the electron density of 0.0004 unit. Here, blue regions represent positive charge; red regions refer to negative charge.

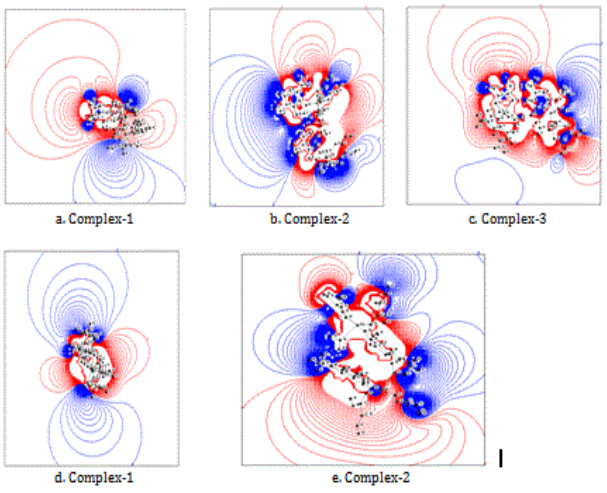

Figure 5: Electrostatic potential of all the complexes a-c (hydrogen bonding arrangement) and d-e (stacking arrangement) mapped onto the surface of the electron density of 0.002 unit.

Bader's Atoms in Molecule theory [28-32]. The interactions were studied by considering the values of the electron density (ρ)its Laplacian ($\nabla^{2\rho}$) and bond ellipticity (ε) at the bond critical points (BCP) of the O-H...O, O–H…N, N-H...N and N-H...O bonds in the metal complexes at M05/LANL2DZ level of theory, and these results are summarized in Table 3. The strong hydrogen bonds are to be linked with large electron density values at the bond critical points (BCPs), leading to high structural stability, and this is observed for all the complexes. In addition, small ellipticity values (e) at the BCPs for all the metal complexes indicate a strong interaction between the atoms. As can be seen from Table 3,

Table 3: The Electron density r (in a.u.) and Laplacian of electron density Ñ2r (in a.u.) and bond ellipticity (e) corresponds to hydrogen bonds in metal interacting complexes (hydrogen bonding and stacking arrangement) calculated through topological analysis and δH- chemical shift of the hydrogen atom (in ppm) at M05/LANL2DZ level of theory

Bonding	ρ	$\nabla^2\rho$	e	**δH**
Hydrogen Bond Arrangement				
Complex 1				
N_{39}-H_{40}...N_8	0.022	0.074	0.049	17.54
N_{15}-H_{76}.....N_{32}	0.045	0.133	0.055	21.75
N_{39}-H_{41}.....O_{57w}	0.016	0.065	0.075	13.9
N_{42}-H_{43}.....O_{57w}	0.036	0.141	0.079	20.68
N_{15}-H_{16}...O_{54w}	0.031	0.112	0.047	16.82
N_{17}-H_{18}...O_{54w}	0.032	0.129	0.096	19.94
O_{22w}-H_{24}....N_{21}	0.076	0.140	0.031	29.28
O_{54w}-H_{56}...O_{67}	0.033	0.137	0.048	9.87
O_{47w}-H_{49}....N_{46}	0.071	0.140	0.034	27.94
O_{54w}-H_{55}...O_{66}	0.010	0.050	0.461	7.11
Cd_7-O_{22}	0.063	0.376	0.088	-
Cd_7-O_{47}	0.062	0.373	0.094	-
Complex 2				
N_{26}-H_{55}...O_{38}	0.011	0.043	0.038	12.98
N_{26}-H_{68}.....O_{20}	0.016	0.062	0.023	12.14
N_{11}-H_{64}.....O_{23}	0.018	0.076	0.047	14.06
C_5-H_{65}....N_{28}	0.015	0.059	0.064	13.74
Cu_{37}-O_{45}	0.041	0.280	0.100	-
Cu_{12}-O_{16}	0.041	0.276	0.108	-
Complex 3				
O_{27}-H_{29}...O_{50}	0.032	0.123	0.024	12.58
N_{40}-H_{41}....O_3	0.021	0.079	0.027	15.1
N_{43}-H_{45}...O_4	0.013	0.055	0.087	15.81
Cu_1-O_{28}	0.069	0.699	0.049	-
Cu_1-O_{27}	0.089	0.550	0.095	-
Cu_{33}-O_{59}	0.266	0.687	0.073	-
Cu_{33}-O_{60}	0.086	0.362	0.052	-
Stacking Arrangement				
Complex 1				
N_{46}-H_{48}...O_{27w}	0.029	0.110	0.061	14.69
N_{49}-H_{50}...O_{27w}	0.028	0.110	0.093	18.8
O_{54}-H_{56}...N_{53w}	0.079	0.134	0.031	29.84
N_{12}-H_{13}...O_{26w}	0.028	0.110	0.093	18.8
N_9-H_{11}...O_{26w}	0.029	0.110	0.061	14.68
O_{17}-H_{19}...N_{16w}	0.079	0.134	0.031	29.84
Cd_1-O_{17}	0.067	0.403	0.089	-
Cd_{38}-O_{54}	0.067	0.403	0.089	-
Complex 2				
N_{22}-H_{24}...O_{31}	0.023	0.081	0.053	10.89
O_{2w}-H_{28}.....N_{40}	0.019	0.058	0.082	5.05
N_1-H_{52}.....O_{61}	0.024	0.093	0.063	8.12
O_{57w}-H_{58}...N_{11}	0.016	0.060	0.041	9.58
Cd_1-O_{17}	0.045	0.292	0.005	-
Cd_{38}-O_{54}	0.046	0.292	0.112	-

the values of (ρ) and ($\nabla^{2\rho}$)for all the metal complexes vary from 0.013-0.079 a.u. and 0.043-0.141 a.u, which proves that the complexes are having strong hydrogen bonds. Also as the ionic radius of the metal cation increases, (ρ) and ($\nabla^{2\rho}$) values of the metal to water oxygen distances are found to decrease from Cu to Cd complexes. In general E(2), the stabilization energy is related to the individual hydrogen bond strength that corresponds to the amount of charge transfer energy at M05/LANL2DZ level of theory and is given in Table 2. It is worthwhile to note that there is a correlation between bond length and stabilization energy E(2), i.e., smaller bond lengths (strong hydrogen bonds) have larger stabilization energy as seen in Table 2.

NMR analysis

The calculation of NMR chemical shielding is an important tool to determine the structures of biomolecules. The relation between the shielding and chemical shift δ is given by,

δ= [(Shielding of carbon/hydrogen in TMS) – (Shielding value of carbon/hydrogen)] (1)

The calculated shielding value for hydrogen atoms in tetramethylsilane (TMS) at MO5/LANL2DZ is 28.49 ppm. By using these values, the δ values corresponding to the respective hydrogen atoms in hydrogen bond interactions have been calculated for all the complexes and are presented in Table 3. It is interesting to note that there is a correlation between bond length and chemical shift, i.e., smaller bond lengths (strong

hydrogen bonds) have larger chemical shift (Figure. 6). During hydrogen bond formation the hydrogen atom loses electrons and gains positive charge, which results in large downfield chemical shift.

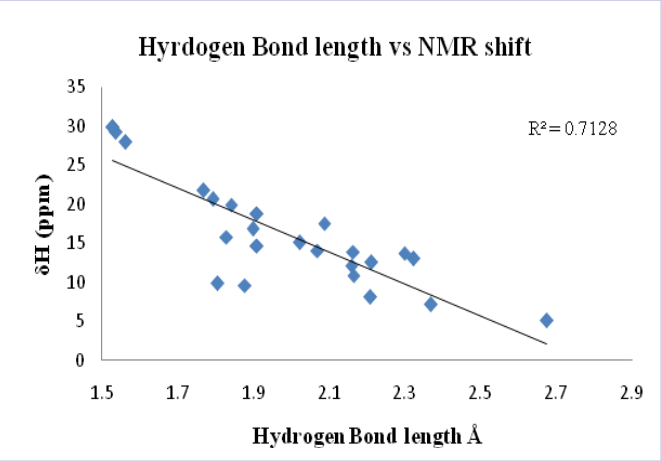

Figure 6: Correlation between the hydrogen-bond length (in A°) and NMR chemical shift δH (ppm) calculated at M05/LANL2DZ level of theory for all complexes

Conclusion

The present study gives better understanding to the metal oxalato complexes by comparing the theoretical and experimental data. The metal complexes of {[Cd(μ-ox) (H ade) (H_2O)]. H_2O}n,{[Cu(μ-ox)(3Meade)(H_2O)].H_2O}n and{[Cu(ox) (H_2O)2(9Megua)].2.5H_2O}n were optimized at B3LYP/LANL2DZ and M05/LANL2DZ levels of theory and to get reliable comparison single point calculations has been carried out at MP2/LANL2DZ level of theory. The calculated geometrical parameters proved that all interatomic bond distances, bond angles and hydrogen bond lengths calculated at the above levels of theory agree well with the X-ray crystallographic data. The presence of hydrogen bond has been identified and studied through the interaction energy. Among the stacking and hydrogen bond arrangement, the interaction energy for the hydrogen bond arrangement is found to be more stable than stacking arrangement indicating the stability of the structure. The electrostatic potential map for hydrogen bonding and stacking arrangement reveals the concentration of the negative charge around the metal oxalato complexes. The results of the topological parameters and stabilization energy give a proper explanation for the stability of the individual hydrogen bonds. The harmonic vibrational analysis clearly indicates very good agreement of O-H, C-H and N-H stretching frequency with the X-ray crystal data. This work can give useful information to understand the conformational damages provoked by the nucleobase N alkylation occurring in biological systems.

Acknowledgments

This work was part of the Research Project (File Number: YSS/2015/000275) and Palanisamy Deepa, is thankful to Science and Engineering Research Board (SERB), Government of India, New Delhi for the award of the Project. Also authors express her sincere thanks to Prof. P. Kolandaivel, Department of Physics, Bharathiar University, and Coimbatore for the computational facility

References

1. Byres M, Cox PJ, Kay G, Nixon E. Supramolecular structures of six adenine-carboxylic acid complexes. CrystEngComm. 2009;11(1):135-142.
2. Galindo MA, Houlton A. Chelate-tethered nucleobases: New architectures and insights in metal ion– nucleobase chemistry. Inorg Chim Acta. 2009;362(3):625-633.
3. Lippert B, Gupta D. Promotion of rare nucleobase tautomers by metal binding. Dalton Trans. 2009;(24):4619-4634. doi: 10.1039/b823087k
4. Navarro JA, Lippert B. Simple 1:1 and 1:2 complexes of metal ions with heterocycles as building blocks for discrete molecular as well as polymeric assemblies. Coord Chem Rev. 2001;222(1):219-250. doi.org/10.1016/S0010-8545(01)00390-3.
5. Hannon MJ. Supramolecular DNA recognition. Chem Soc Rev. 2007; 36(2):280-295. doi:10.1039/B606046N.
6. Lippert B. Multiplicity of metal ion binding patterns to nucleobases. Coord Chem Rev. 2000;200-202,487-516. doi.org/10.1016/S0010-8545(00)00260-5.
7. Lippert B. Metals in medicine. John Wiley and Sons: New York: 2005.
8. Terrón A, Fiol JJ, García-Raso A, Barcelo-Oliver M, Moreno V. Biological recognition patterns implicated by the formation and stability of ternary metal ion complexes of low-molecular-weight formed with amino acid/peptides and nucleobases/nucleosides. Coord Chem Rev. 2007;251(15-16):1973-1986. doi.org/10.1016/j.ccr.2007.03.006
9. Choquesillo-Lazarte D, Brandi-Blanco MdP, Garcia-Santos I, Gonzalez-Perez J, M Castineiras A, Niclos- Gutierrez J. Interligand interactions involved in the molecular recognition between copper(II) complexes and adenine or related purines. Coord Chem Rev. 2008;252(10-11):1241-1256. doi.org/10.1016/j.ccr.2007.09.018.
10. Miguel PS, Amo-Ochoa P, Castillo O, Houlton A, Zamora F, Hadjiliadis N, et al. Chapter 4. Supramolecular Chemistry of Metal–Nucleobase Complexes. Blackwell-Wiley: 2009.doi: 10.1002/9781444312089.ch4.
11. Castillo O, Luque A, Garcia-Teran JP, Amo-Ochoa P. 9. Molecular Recognition Process between Nucleobases and Metal-Oxalato Frameworks. 2009;9:407-449. doi: 10.1002/9780470527085.ch9
12. Verma S, Mishra AK, Kumar J. The Many Facets of Adenine: Coordination, Crystal Patterns, and Catalysis. Acc Chem Res. 2009;43(1):79-91. doi:10.1021/ar9001334.
13. Desiraju G, Steiner T. The weak hydrogen bond: in structural chemistry and biology. Oxford Science Publ: 1999.
14. Janiak CJ. A critical account on π–π stacking in metal complexes with aromatic nitrogen-containing ligands . Chem Soc Dalton Transactions. 2000,(21):3885-3896. doi: 10.1039/B003010O
15. Mukhopadhyay U, Choquesillo-Lazarte D, Niclos-Gutierrez J, Bernal I. A critical look on the nature of the intra-molecular interligand π,π-stacking interaction in mixed-ligand copper(II) complexes of aromatic side-chain amino acidates and α,α′- diimines. CrystEngComm. 2004;6(102):627-632. doi: 10.1039/B417707J
16. Nishio M. CH/π hydrogen bonds in crystals. CrystEngComm.

2004;6(27):130-158. doi: 10.1039/B313104A

17. Jiang YF, Xi CJ, Liu YZ, Niclos-Gutierrez J, Choquesillo-Lazarte D. Intramolecular "CH•••π (Metal Chelate Ring) Interactions" as Structural Evidence Metalloaromaticity in Bis(pyridine-2,6-diimine) Ru II omplexes. Eur J Org Chem. 2005;(8):1585-1588.doi:10.1002/ejic.200400864

18. Garcia-Teran JP, Castillo O, Luque A, Garcia-Couceiro U, Beobide G, Roman P. Molecular Recognition of Adeninium Cations on Anionic Metal–Oxalato Frameworks: An Experimental and Theoretical Analysis. Inorg Chem 2007;46(9):3593-3602.doi: 10.1021/ic062448s

19. Dance I, Scudder M. Supramolecular motifs: sextuple aryl embraces in crystalline [M(2,2′-bipy)3] and related complexes. J Chem Soc Dalton Transactions 1998;(8):1341-1350. doi: 10.1039/A707237F

20. Perez-Yanez S, Castillo O, Cepeda J, Garcia-Teran JP, Luque A, Roman P. Supramolecular architectures of metal–oxalato complexes containing purine nucleobases. Inorg Chim Acta. 2011;365(1):211-219. doi: 10.1016/j.ica.2010.09.012

21. Garcia-Terán JP, Castillo O, Luque A, Garcia-Couceiro U, Beobide G, Roman P. Molecular Recognition of Protonated Cytosine Ribbons by Metal– Oxalato Frameworks. Cryst Growth Des. 2007;7(12):2594-2600. doi: 10.1021/cg0705916

22. Garcia-Teran JP, Castillo O, Luque A, Garcia-Couceiro U, Beobide G, Roman P. Supramolecular architectures assembled by the interaction of purine nucleobases with metal-oxalato frameworks. Non-covalent stabilization of the 7H-adenine tautomer in the solid-state. Dalton Transactions. 2006; (7):902-911. doi: 10.1039/B510018F

23. Garcia-Teran JP, Castillo O, Luque A, Garcia-Couceiro U, Roman P, Lloret F. One-Dimensional Oxalato-Bridged Cu(II), Co(II), and Zn(II) Complexes with Purine and Adenine as Terminal Ligands. Inorg Chem. 2004;43(18):5761-5770. doi: 10.1021/ic049569h

24. Wyatt MD, Allan JM, Lau AY, Ellenberger TE, Samson LD. 3-Methyladenine DNA glycosylases: structure, function, and biological importance. BioEssays. 1999;21(8):668-676.doi: 10.1002/(SICI)1521- 1878(199908)21:8<668::AID-IES6>3.0.CO;2-D

25. Deepa P, Kolandaivel P. Studies on Tautomeric Forms of Guanine-Cytosine Base Pairs of Nucleic Acids and Their Interactions with Water Molecules. J Biomol Struct Dyn. 2008;25(6):733-746. doi.org/10.1080/07391102.2008.10507217

26. Deepa P, Kolandaivel P, Senthilkumar K. Interactions of anticancer drugs with usual and mismatch base pairs - Density functional theory studies. Biophys Chem.2008;136(1):50-58. doi.org/10.1016/j.bpc.2008.04.007

27. Deepa P, Kolandaivel P, Senthilkumar K. Structural Properties and the Effect of 2, 6-Diaminoanthraquinone on G-Tetrad, Non-G-Tetrads, and Mixed Tetrads-A Density Functional Theory Study. Int J Quant Chem. 2011;111(12):3239-3250. doi: 10.1002/qua.22720

28. Deepa P, Kolandaivel P, Senthilkumar K. Theoretical investigation of interaction between Psoralen and Altretamine with stacked DNA base pairs. Mat Sci Eng C. 2012;32(3):423-431doi.org/10.1016/j.msec.2011.11.014

29. Deepa P, Kolandaivel P, Senthilkumar K. Hydrogen bonding studies of Amino acid side chains with DNA base pairs. Mol Phys. 2011;109(16):1995-2008. doi.org/10.1080/00268976.2011.602649

30. Deepa P, Kolandaivel P, Senthilkumar K. First and second coordination spheres in 8-azaxanthinato salts of divalent metal aquacomplexes – Ab initio and DFT study. Polyhedron. 2011;30(9):1431-1445. doi.org/10.1016/j.poly.2011.01.018

31. Deepa P, Kolandaivel P, Senthilkumar K. Structural properties and the effect of interaction of alkali (Li+, Na+, K+) and alkaline earth (Be2+, Mg2+, Ca2+) metal cations with G-tetrad and SG-tetrads. Comput Theor Chem. 2011;974(1-3):57-65. doi.org/10.1016/j.comptc.2011.07.012

32. Deepa P, Kolandaivel P, Senthilkumar K. Structural properties and the effect of platinum drugs with DNA base pairs. Struct Chem. 2013;24(2):583-595. doi: 10.1007/s11224-012-0087-y

33. Zhao Y, Schultz NE, Truhlar D. Exchange-correlation functional with broad accuracy for metallic and nonmetallic compounds, kinetics, and noncovalent interactions. J Chem Phys. 2005;123(16):161103. doi: 10.1063/1.2126975

34. Hay PJ, Wadt WR. Ab initio effective core potentials for molecular calculations. Potentials for K to Au including the outermost core orbitals. J Chem Phys. 1985;82(1):299. doi.org/10.1063/1.448975

35. Wadt WR, Hay PJ. Ab initio effective core potentials for molecular calculations. Potentials for main group elements Na to Bi . J Chem Phys.1985;82(1):284. doi.org/10.1063/1.448800

36. Boys SF, Bernardi FD. The calculation of small molecular interactions by the differences of separate total energies. Some procedures with reduced errors. Mol Phys 1970;19(4):553-566. doi.org/10.1080/00268977000101561

37. Bader RFW. Atoms in Molecules - A Quantum Theory, Oxford University Press, Oxford, 1990. ISBN: 0198558651.

38. Popelier P. Bader R. The existence of an intramolecular CHO hydrogen bond in creatine and carbamoyl sarcosine. Chem Phys Lett 1992;189(6):542-548. doi.org/10.1016/0009-2614(92)85247-8

39. Cheeseman J, Carroll M, Bader R. The mechanics of hydrogen bond formation in conjugated systems. Chem Phy Lett 1988;143(5):450-458. doi.org/10.1016/0009-2614(88)87394-9

40. Carroll MT, Chang C, Bader RF. Prediction of the structures of hydrogen-bonded complexes using the laplacian of the charge density. Mol Phys.1988;63(3):387-405. doi.org/10.1080/00268978800100281

41. Koch U, Popelier P. Characterization of C-H-O Hydrogen Bonds on the Basis of the Charge Density. J Phys Chem. 1995;99(24):9747-9754. doi:10.1021/j100024a016

42. Glendening E, Reed A, Carpenter J, Weinhold F. NBO 3.1.University of Wisconsin, Madison. 1998.

43. Cheeseman JR, Trucks GW, Keith TA, Frisch MJ. A comparison of models for calculating nuclear magnetic resonance shielding tensors. J Chem Phys. 1996,104(4):5497. doi.org/10.1063/1.471789

44. Frisch MJGW, Schlegel HB, Scuseria GE, Robb MA, Cheeseman JRZVG, Montgomery JA, etal. Gaussian 09. Revision A.11.2, Gaussian, Inc. Pittsburgh PA, 2005.

45. Garcla-Couceiro U, Castillo O, Luque A, Garcia-Teran JP, Beobide G, Roman P. One-Dimensional Oxalato-Bridged Metal (II) Complexes with 4-Amino-1,2,4-triazole as Apical Ligand. Eur J Inorg Chem. 2005;2005(21):4280-4290. doi: 10.1002/ejic.200500332

46. Imaz I, Bravic G, Sutter JP. Structural and zeolitic features of a series of supramolecular porous architectures based on tetrahedral {M(C2O4)4}4– primary building units. Dalton Transactions. 2005;(16):2681-2687. doi:10.1039/B503964A

47. Chin K, Sharp KA, Honig B, Pyl, AM. Calculating the electrostatic properties of RNA provides new insights into molecular interactions and function. Nat Struct Mol Biol. 1999;6(11):1055-1061. doi:10.1038/14940